RSC Advances

ROYAL SOCIETY OF CHEMISTRY

www.rsc.org/advances

Dual-tuning multidimensional superstructures based on a T-shape molecule: vesicle, helix, membrane and nanofiber-constructed gel

Xiaoxiao Chu[a], PengyaoXing[a], ShangyangLi[a], MingfangMa[a], Jingcheng Hao[a] andAiyouHao[1a]

[a]*School of Chemistry and Chemical Engineering and Key Laboratory of Colloid and Interface Chemistry of Ministry of Education, Shandong University, Jinan 250100, PR China.*

1 Fax: +86 531 88564464; Tel: +86 531 88363306; E-mail: haoay@sdu.edu.cn.

Abstract:

As a small molecule, N-(9-Fluorenylmethoxycarbonyl)-glycine (FG) possesses a hydrophobic plane domain (π-conjugated section) and a hydrophilic domain (amino acid section), which can be designed into multi-dimensional self-assembly structures under dual tunings. Through controlling the concentration of T-shape FG, the transformation between various morphologies have been achieved: vesicles are obtained at low concentrations (0.0025~0.005 wt%); helical fibers can be found at the concentration of 0.2 wt% though Gly has no stereocenter, resulting in a birth of chiral organization; fibrous bundles can accumulate into three dimensional network to finally form supramolecular gel. Taking an example of gel, we devised a variety of nanostructures including nanoparticle, microparticle, nanoribbon and membrane gotten by adding base. The mechanism of self-assembly formation has been investigated and this system is hoped to enrich the category of nanomaterials from amino acid or short peptides.

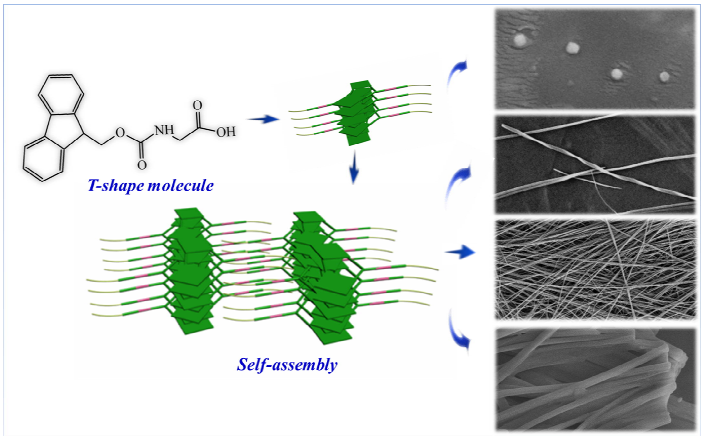

Keywords: multi-dimension, dual-tuning, nanostructures, self-assembly

1 Introduction:

Recently, multi-dimensional self-assemblies have attracted much attention, due to the ability of producing well-defined architectures, which have great applications, such as in nanomaterials, drug release, catalysis and biosensor.[1] The manifestation of functions of these materials is based on the various morphologies (0-D vesicle or solid

sphere, 1-D nanotube or helix, 2-D membrane and 3-D gel network) to some extent. For example, amphiphilic molecule has the ability of forming micell or vesicle.[2] The hermetic bilayer of vesicle can allow a hydrophilic cavity to entrap suitable active molecule.[3] Through controlling the aggregation/disaggregation behaviors of vesicle, one can achieve drug release/delivery, enhanced solubilizing effect, embedding function.[4] Another example is the nanotube or nanofiber (1D) which shows favorable properties, achieving functions in constructing transmembrane channel, making microelectron, encapsulation, medicine.[5] Moreover, the helical fiber (1D) gives a deeper insight into the specific interactions between functional molecules.[6] Especially, π-conjugated molecules are the building blocks of solid-state architectures to self-assemble hierarchically into nanotubes.[7] For planar membrane, the fascinating properties have a wide application in biocatalytic template, transfer information, molecular recognition.[8] Finally, as a representative supramolecular bulk phase, gels constituted by a 3D network of fibers by encapsulating solvent under the capillary forces. Meanwhile, intermolecular interactions endow gel with many unique properties such as shape memory, self-healing, biocompatibility and solid-like strength to be applied in the biological culture.[9]

During the procedure of the construction, noncovalent interactions, such as hydrogen bonding, π-π stacking, Vander Waals interactions or metal-ligand coordination play key roles in the self-aggregation behaviors.[10] It is also worth to note that supramolecular materials are more convenient in realizing stimuli-responsiveness than the conventional materials as the presence of the reversible non-covalent bonds. The responsive property makes it easier to design materials with morphological and dimensional changes. In addition, different solvent environments have influences on the formation, mechanical strength, nanomorphologies of supramolecular assemblies.[11] Although supramolecular gel includes two major categories depending on solvent: organic solvent and water solvent, organo-hydro (or hybrid) solvent displays a special forming process by mixing an organic solvent and water solvent relying on good/poor solvent strategy.

In nature, amino acid and oligopeptide, as small bioactive molecules, are of great significance in the life system because of the biological compatibility and imported functional groups.[12] Multiple nanostructures which possess sensitive responsiveness: pH, temperature, concentration, redox, mechanical force and light can be spontaneously fabricated by the supramolecular molecules designed through appending various functional groups on building blocks.[13] An important feature of amino acid assembly is the functional group of amide, and the driving forces including hydrophobic/hydrophilic interactions and intermolecular hydrogen bonds (H-bonds) are the keys for self-aggregation behaviors. More importation of functional groups (fluorenylmethoxy carbonyl, anion/cation and linear molecule) brings up the self-assembly with diverse morphologies and functions. Scientists have built well-defined nanomaterials in water via the self-assembly of amino acid, amphiphiles, π-conjugated molecules.[14] A few successful works leave no doubt about the influence of amino acid-containing gel in supramolecular self-assembly.[15] Nonetheless, it is a big challenge to tuning about the formation of materials, including dimension, size and strength. And a unique approach to achieve responsive self-assembly of a sole molecule at low concentration by simple mixed approach (below 5 wt%)were rarely reported.

Here, we report a simple way to design multidimensional self-assembly based on a small bioactive molecule. FG, a special T-shape amphipathic molecule, was used as the sole device bearing an aromatic plane group (conjugated group) and amino acid group. Upon tuning of the FG concentration, vesicles, helical ribbons, a 3D network of molecular gels was successively manufactured. Self-assembly behavior brought about not only various controllable morphologies, but also the birth of chiral assembly. What's more, it was straightforward to make a molecular gel for further study. So we chose a well-defined gel to investigate the responsiveness of base. The 3D network of gel was transformed into the morphologies with different dimensionalities such as nanoparticles, microparticles, bamboo-like fibers and membrane upon the addition of base. These attractive benefits leaded us to construct the self-assembled structures

based on bioactive small molecules. We deeply studied the forming process of multiple morphologies, special properties of self-assembly structures and proved some novel understanding of the natural mechanism of molecular arrangement. Dual-tuning nano/micromaterials with different dimensionalities were designed, displaying potential applications in biosensor, smart materials and cell scaffold.

2 Experimental sections:

2.1 Materials

N-fluorenyl-9-methoxycarbonyl glycine acid was purchased from Aladdin Chemical Reagent Co. Ltd., Shanghai, China. All the other reagents were purchased from Country Medicine Reagent Co. Ltd., Shanghai, China to AR grade. All the reagents were used without further purification.

2.2 The preparation of the samples

All the samples were prepared according to different ethanol-water solvent ratios from 1/9 to 9/1 (v/v). A certain amount of FG was dissolved into ethanol to get a transparent solution and then water was added to the solution under ultrasonic conditions. A series of self-assembly systems were formed at different weight concentration of FG.

Gel containing 1 wt% gelator was chosen for further study of base responsiveness because of its good mechanical properties and stability at room temperature. When different amount of NaOH was added into the gel, a variety of phenomenas were observed. Finally, Transmission Electron Microscopy (TEM) was used to study the stimuli-responsiveness of these gel systems.

2.3 Characterization

Samples were stained by the phosphotungstic acid for TEM and measured through a JEM-100CX II electron microscope (100 kV). Dry samples were kept in vacuum desiccators for 24 h and the microstructures of the samples were studied by Field-emission scanning electronic microscopy (SEM, ZEISS SUPRA 55). Optical pictures were obtained under optical microscopy (OM) by adjusting the focal length and magnifying multiple with enough apertures. UV-vis spectra were recorded at

room temperature with a TU-1800pc UV-vis spectrophotometer. Cell length was fixed as 0.1 mm. Samples were measured on a German Bruker/D8 ADVANCE diffractometer with Cu Kα radiation (λ= 0.15406 nm, 40 KV, 40 mA) for X-ray diffraction (XRD) experiments. Helix fibers were measured at room temperature with a JASCO-J810 Circular Dichroism Spectrometer for circular dichroism (CD) spectra. A Thermo Haake RS6000 rheometer was used to study the rheological properties of wet gels. The thermal gravity analysis (TGA) and differential scanning calorimetry (DSC) thermogram were recorded with the temperature ranging from 80 to 350 °C at the heating rate of 10 °C/min under a N_2 atmosphere with the reference of empty aluminum. Dynamic light scattering (DLS) was done for the grain size of samples. The sample solution was prepared by filtering under a 450 nm millipore filter into a clean scintillation vial. The optimized molecular models are drawn by the software Materials Studio 5.5 by Accelrys.

3 Results and Discussion:

3.1 Self-assembly behavior of FG molecule

The multifarious self-assemblies of FG (Fig. 1a) were fabricated by adding different amounts of FG ethanol solution into distilled water through good/poor solvent strategy.[16] This molecule contains a hydrophobic plane part and a hydrophilic amino acid part formed threadlike fibers (Fig. 1c left) with certain orientation (Fig. 1b) at low concentration through observing the optical microscope image under polarized light. With the increase of FG concentration, a series of supramolecular gels were generated at room temperature. The gel gradually (Fig. 1c middle) presented a semitransparent view and Fig. 1c right displayed a white gel. So the self-assembly behavior of FG exhibited a concentration-dependent impact with different bulk phases.

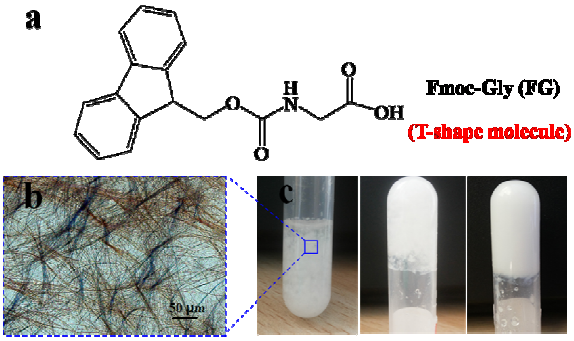

Fig. 1 a) Molecular formula of FG, b) the optical microscope image of the complete sample under polarized light, c) the optical images of FG at different concentrations (from left to right: C_{FG} = 0.2 wt%, 0.5 wt%, 1 wt%; ethanol/water (v/v) = 3/7).

In order to show the process of self-assembly, the concentration of FG and the ratio of ethanol/water are two key factors to control the formation of the self-assemblied structures.[17] Generally, the weight percent of the gelator kept below 10 %. As shown in Fig. 2, multiple self-assembly behaviors can be observed in the solvent volume ratio from 3/7 to 5/5. Dotted circle shows the possible area of vesicle (0.0025 ~ 0.005 wt%). The range of gel formation depends on the comprehensive effect between the concentration of FG and the volume ratio of mixed solvents. The solutions at low concentration (0.1 ~ 0.2 wt%) of FG could be easy to form gel even if the solvent volume ratio was small (1/9 ~ 2/8), which confirmed the fact that water was an induced factor in gel formation.[18] Obviously, high concentration of FG is conducive to the formation of gel and the solvent ratio can be loosened accordingly. Other areas of the Fig. 2 include solution, floccus and precipitate.

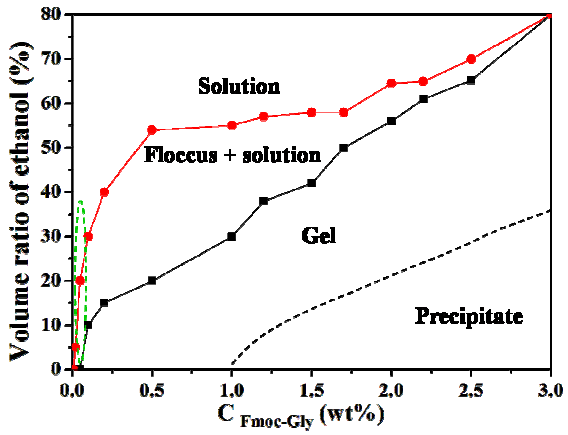

Fig. 2 Phase diagram of the system. Dashed line: speculated boundary of gel and

precipitate; dashed circle: possible range of vesicle.

3.2 Morphological studies

TEM and SEM were employed for investigating the morphologies of the self-assembly. In Fig. 3a, the uniform nanoparticles can be observed as a 0D structure and the size is about 200 nm. From the enlarged view, the hollow shell proves the nature of vesicle which can be observed with different degree of darkness. Furthermore, the DLS characterization gives an average hydrodynamic radius (R_h) of 201.5 nm (Fig. 3b) which also reveals the vesicle structure at low concentration.[19]

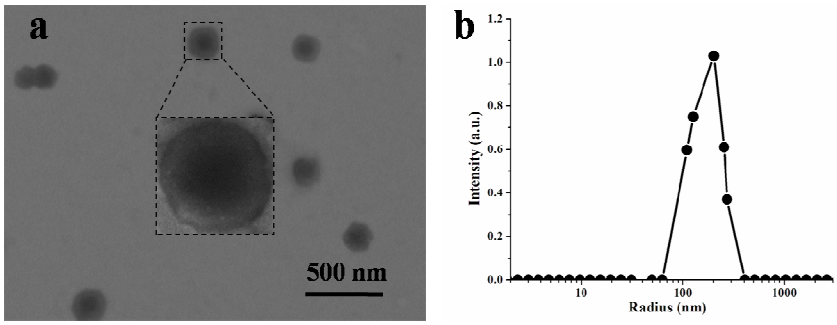

Fig. 3 a) TEM image of the sample (C_{FG} = 0.005 wt%, ethanol/water (v/v) = 3/7), b) DLS distributions of the sample.

On the middle concentration range (e.g. 0.2 wt%), loosely packed nanofibers will be given. As shown in Fig. 4a, we surprisingly observed the presence of helical ribbons in spite of the absence of stereocenter of glycine.[20] Clearly, the stacking of Fmoc moieties play a vital role in determining the twisted structure in a molecular scale. The original solution was injected into water under ultrasound and the mixed system was deposited at room temperature, then the helical fibers grew up gradually. So the fibers look threadlike under the enough space environments (Fig. S1). Generally, the supramolecular helical structure derives from chiral amplification, which means the transfer of molecular conformational chirality to morphological chirality in the overall superstructure. But for achiral molecules, the process of forming super-chirality, as called symmetry breaking, is based on the subtle intermolecular interactions among building blocks. In this mode, the molecular aggregation with some molecular angles in certain orientations may be caused by some space (steric hindrance) or orientational

interactions factors. Especially, the hydrogen bonding, as a highly directional non-covalent interaction, has a profound influence on the molecular arrangement.[21] Proof for the helical structure comes from the CD spectrum of the system containing 0.2 wt% FG compared with those containing 0.005 wt% or 2 wt% FG. The helical fibers show left- (M) or right-handed (P) twists, which can be measured by CD spectrum. The strong negative signal verifies the super-chiral assembly at 0.2 wt% FG (Fig. 4b) belongs to left- (M) twist, which is coincided with the result of SEM. To further demonstrate the formation process of the helical fibers, time-dependent optical microscope images were employed. We can find the submicron particles occur first and then the short fibers appear. Finally, the vimineous fibers extend in 1D up to hundreds of micrometers or even longer which provides some evidence for subsequent analysis of forming mechanism (Fig. S2).[22] In spite of the T-shape molecule without chirality, the birth of chiral fibers may be induced by the constituent amino acid. What's more, the π-π stacking assembly is expanded by these helical fibers. The hydrophilic part and Fmoc aromatic part can control the twisting ability of self-assembly in our systems. This causes the molecules to rotate at different angles relative to each other, thereby resulting in the formation of the optimum molecular geometry with a molecular twist. The substituent of amino acid in peripheral positions results in an overcrowded environment during stacking, thus leading to an uneven symmetry breaking and the formation of chiral assemblies.[21]

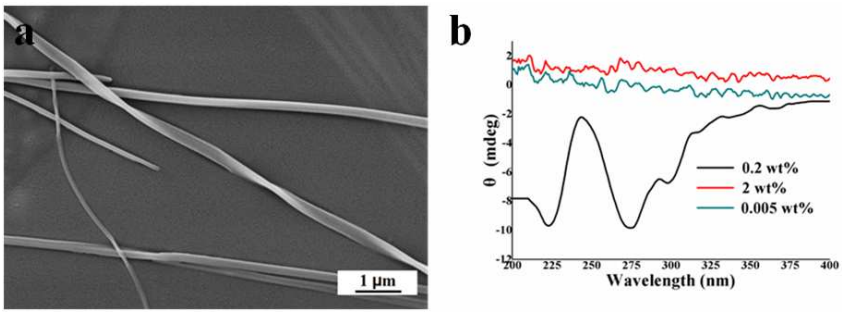

Fig. 4 a) TEM image of the helical fibers (C_{FG} = 0.2 wt%, ethanol/water (v/v) = 3/7), b) CD spectrum of the helical fibers.

The TEM (Fig. 5a) and SEM (Fig. 5b) images reveal that the 3D network is composed

of 1D nanofibers with the increase of the FG concentration.[23] Inset in Fig. 5a displays a rigid and free-standing gel-like structure. It is interesting that the helical fibers change to the clusters of wires and fibers after increasing the FG concentration. To further elucidate the properties of the supramolecular system, we performed rheological measurement to study the viscoelasticity of the gel. The dynamic oscillatory stress sweep image (Fig. 6) shows the characteristic of supramolecular gel of which storage modulus G' is higher than the loss modulus G".[24] The G' (~ 4000 Pa) at 0.5 or 1 wt% FG concentration is high enough to show the strong mechanical strength of the gel and the G' is about ten folds than the G" which corroborates the gel is composed of well-behaved structure.[25] It should be noted that, after increasing the concentration of FG, although the gel owes the higher density, we could hardly find the presence of helical fibers. Only rigid, straight and bounded fibers are given. Definitely, concentration-dependent complex pathways control the self-assemblies of FG in mixed solvent environment, generating diverse phases and nanostructures.

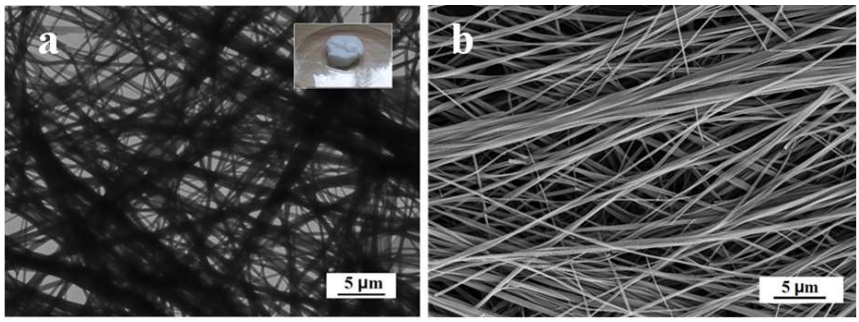

Fig. 5 TEM (a) and SEM (b) images of the supramolecular gel (C_{FG} = 1 wt%, ethanol/water (v/v) = 3/7), inset: optical image of the gel.

It is noteworthy that the system with 0.2 wt% FG is similar to a gel of which the G' is larger than the G" (Fig. 6a). Nevertheless, it is a gellike because it can flows with inversion test. We suspected that it is a transition state between solution and gel fibers. On account of the weak strength, the gellike of 0.2 wt% FG could not be stable for the properties of gel owing to the deficiency of fiber density. Frequency sweep of rheological measurements was carried out to study the strength of the gel.[26]

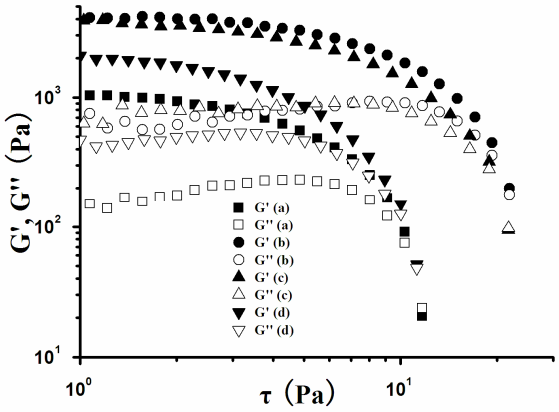

Fig. 6 Dynamic oscillatory stress sweep of the samples at different concentrations of FG (a, 0.2 wt%; b, 0.5 wt%; c, 1 wt%; d, 2wt%; ethanol/water (v/v) = 3/7).

As shown in Fig. 7, smooth curves display the stabilities of the gels following the change of rotational frequency. All the G' at about 1000 Pa proves the gels possess well mechanical strength. Fig. 7 has no curve about the 0.2 wt% FG-containing system, corroborating aforementioned observations. What's more, the gel (Fig. S3) immediately forms when mixing the solution of 2 wt% FG and water, which is different from the gradual process of the gel formation with 0.5 or 1 wt% FG. From the data of Fig. 6d and Fig. 7c, the gel formed by 2wt% FG is weaker than the gel with 0.5 or 1 wt% FG, which may be a crystal-like gel with short fibers.[27]

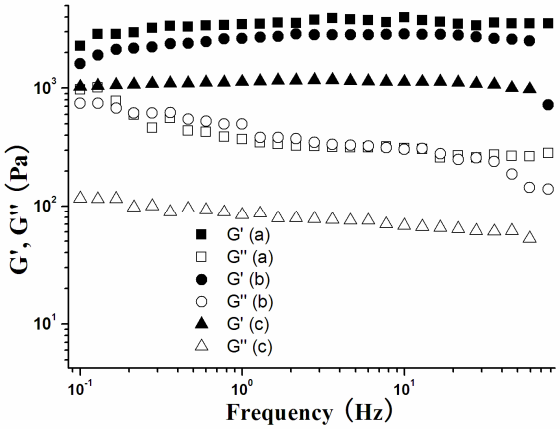

Fig. 7 Frequency sweep of the samples at different concentrations of FG (a, 0.5 wt%; b, 1 wt%; c, 2 wt%; ethanol/water (v/v) = 3/7).

The optical microscope image under polarized light is not only powerful technique for

measuring the microsturcture of system, but also simple method of providing the molecular arrangement.[28] As shown in Fig. 8, some well-oriented morphologies are confirmed by the strong birefringence. The gel fibers exhibit a high ordered structure which suggests the sol-to-gel transition enables the FG molecules to aggregate along the specific direction driven by the intermolecular interactions.[29] The one-dimensional orientation of FG improves the color and anisotropic properties. The consequence that long fibers (Fig. 8a, b) are formed at low concentration and the short fibers are formed (Fig. 8c, d) at high concentration is consistent with the data of rheology.[30] On the one hand, the aggregation of FG molecules with specific orientation at low concentration is easy to emerge helical and long fibers tardily at low concentration. The free degree of molecules tends to decrease with an increase of the concentration because the intermolecular interactions, especially π-π stacking, hydrogen bonding and the intermolecular space resistance, become obvious and strong.[31] So the fibers in Fig. 8c, d display shorter appearance but more luminous color than the fibers in Fig. 8a, b. On the other hand, the time of the self-assembly formation is also a key of the strength and morphology of system.[32] In Fig. 8a, b, the gel fibers are shaped tardily and the FG molecules have enough time to germinate along the certain directions. However, the gels (Fig. 8c, d) formed immediately by mixing FG solution and water are not provided enough time to grow freely. So the fibers exhibit short and are only focused on the limited directions. As shown in Fig. S3, the whole fibers are like the conglutination of the straight and thin fibers which are similar to the helical fibers in size (Fig. S1).

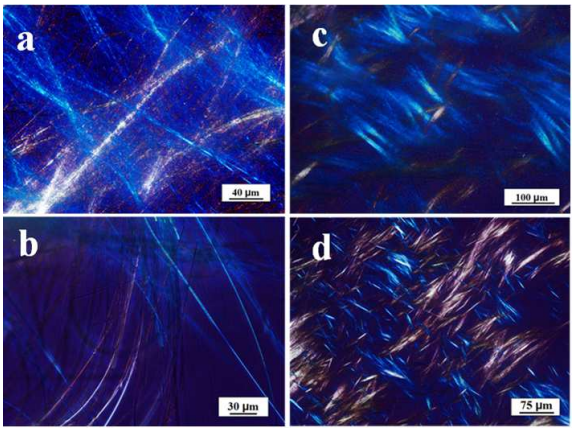

Fig. 8 Optical microscope images at different concentrations of FG (a, 0.5 wt%; b, 1wt%; c, 2 wt%; d, 3 wt%; ethanol/water (v/v) = 4/6) under polarized light.

3.3 Mechanism studies

To understand the thermal stability and molecular self-assembly, DSC curves were detected for pure FG and dried self-assembly samples.[33] As shown in Fig. 9, an endothermic peak in the curves of the dried samples is found at 100 ° C (the boiling point of water), which is from the evaporation of water. Without the pure FG molecule, the curves of the dried self-assembly samples have two small endothermic peaks (the range: 120 ~ 160 °C, marked by the dashed line), which indicates the thermal stability of the systems has been modified by the intermolecular interactions, such as π-π stacking and hydrogen bonding. Meanwhile, there are two strong endothermic peaks (~175 °C, ~265 °C) in each curve. They are from the degradation of the carboxyl and hydroxyl groups and the separation of π-π plane.[34] The pure crystal owns the excellent thermal stability because of its structured and ordered arrangement of molecule. So the two peaks have the respective highest temperature (dotted lines). What's more, we can find that the peaks of the self-assembly shift more closely to the corresponding peak of the pure FG molecule at high FG concentration. Therefore, the self-assembly process promotes the transform of sol-gel and improves the thermal stability.[35] Compared with the helical fibers at 0.2 wt% FG, the gels (0.5, 1 wt% FG), a 3D network of gel fibers filled with solvent, are closed to the solid crystal, which is consistent with the properties of rheological measurements. These gels possess strong strength and well-ordered orientation of molecules. It maybe provides a new approach to designing a temperature-responsive material.

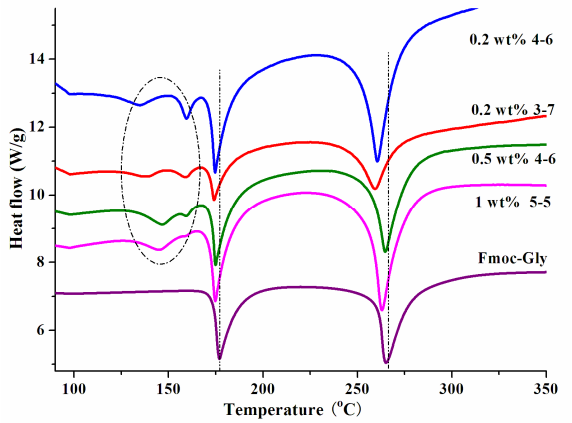

Fig. 9 DSC curves of dried samples at different concentrations of FG and solvent ratios.

UV-vis spectra provide information regarding the aggregation of fluorophores. There are two strong absorption peaks of FG in Fig. 10. Compared with the curve of the FG solution, the spectrum of the self-assembly samples have tiny blue shift of the absorption peaks from 264 nm to 262 nm.[36] So the blue shift indicates the existence of intermolecular interaction between aromatics. Secondly, another blue shift from 298 nm to 294 nm deeply represents a strong intermolecular conjugation which is most likely due to the face-to-face type π-π stacking of the Fmoc functional group.[37] Finally, the curve of the gel at 0.5 wt% FG has an obvious absorption at 310-370 nm, it can be explained by the formation of gel which show a certain turbidity.

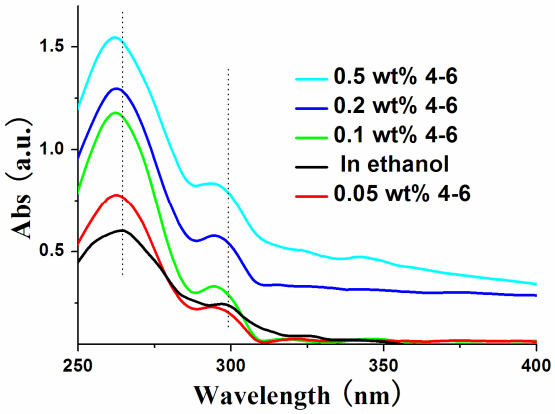

Fig. 10 UV-vis spectra of the samples at different concentrations of FG with the same solvent of 4/6 (v/v).

3.4 The morphological changes by adding base

In an effort to investigate more responsiveness of the FG self-assembly system, we chose a well-behaved and stable gel (1 wt% FG) to study deeply. TEM in Fig. 11 commendably illustrates the appearance changes of the gel (Fig. 5) switched by the addition of base. As shown in Fig. 11a, A little amount of base is just like a trigger to cut off the gel fibers (like bamboo leaves). Then, the fiber-containing 3D network disappears and the flocculent membrane (2D structure), interspersed by nanoparticles, covers the entire field of vision (Fig.11b) when added suitable base.[38] Finally, the gel fibers are dissociated to big particles with the addition of the excess base (Fig. 11c). It seems that the base breaks up the hydrogen bonding between FG molecules, inducing the disaggregation of the gel fibers: firstly, shorter fibers; secondly, thinner floccules; finally particles, which is contrary to the time-dependent process of self-assembly.[39] The multifarious morphologies induced by base are worthy of the further study in biological tissue field.

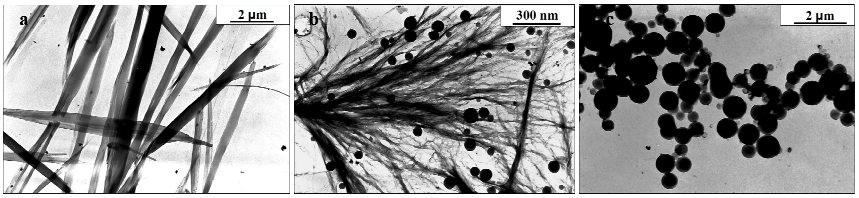

Fig. 11 TEM images of the samples (FG concentration is 1 wt%, solvent volume ratio is 3/7) with the addition of base (NaOH: a 0.2 g, b 0.005 g, c 0.001 g).

3.5 The molecular arrangements

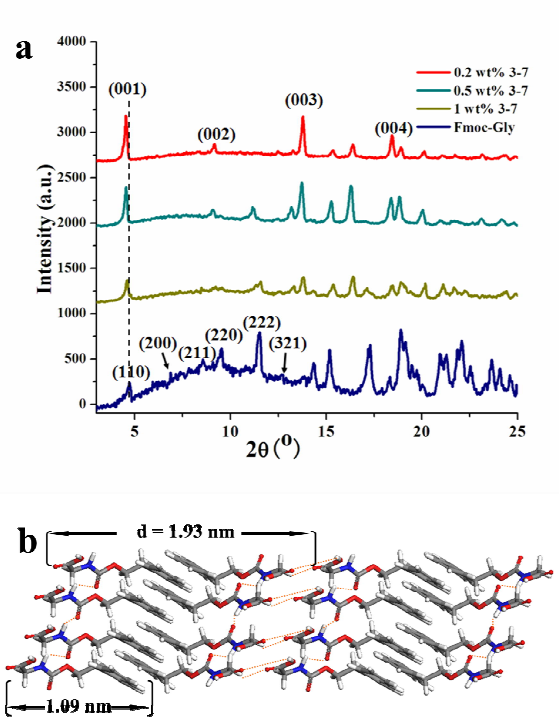

Fig. 12 a) XRD patterns of FG and the dried self-assembly structures, b) molecular simulation diagram.

To explore the essential mechanism of the self-assembly behavior, XRD was performed to supply the information of the molecular microstructure.[40] The diffraction pattern displays a series of peaks. The first intense reflection at $2\theta = 4.7^{\circ}$ corresponds to a calculated *d* spacing of 1.8 nm. The ratios of $\sin^2\theta$ are consistent with the parameters of body-centered cubic so the initial six lattice planes can be marked in Fig. 12a. Meanwhile, when the molecules self assembly at the concentration of 0.2 wt% FG, the XRD pattern shows that the four major peaks at 4.5, 9.2, 13.8, 18.5 ° of which the ratio of *d* spacing are calculated as 1:1/2:1/3:1/4. It proves the presence of lamellar structure formed by the parallel stacking along their long single fibrils.[41] From Fig.12b, we can obtain that the interlayer spacing is 1.93 nm smaller than the twice of the molecular size (1.09 nm). Because the π-π stacking engenders the overlap of molecule and the interspace between layers also changes the *d* spacing. The first peak shifts to the smaller angle, indicating that the self-assembly structures are looser than the FG crystal. With the increase of the FG concentration, the lamellar stacking is

more close to the crystal arrangement of initial FG, which is from that XRD pattern emerges more peaks like in pure crystal and the first peak approaches to crystal.[42] There is a transition state (gel) from helical fibers to crystal. All of these are in conformity with the above discussions.

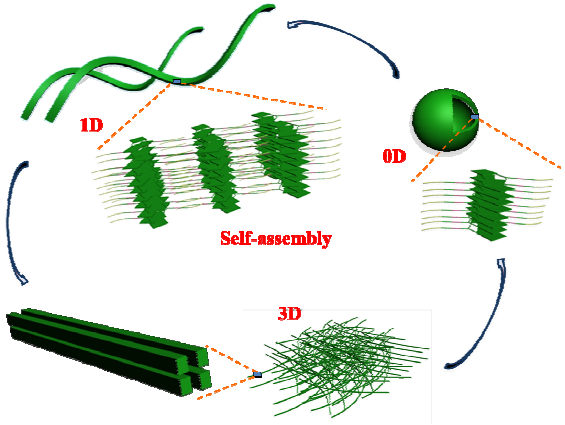

Fig. 13 Schematic representation of the concentration-dependent self-assembly mechanism.

So we propose a mechanism of the self-assembly behavior in multidimensional structures (Fig. 13). The FG molecules form a dual-hydrophilic dimer by π-π stacking and the vesicles (0D) are composed of the cumulate dimmers induced by water at low concentration.[43] The intermolecular interactions, especially hydrogen bonding, increase with the increase of the FG concentration (about 0.2 wt%). The combination of π-π stacking and hydrogen bonding enhance the ability of molecular arrangement.[44] Due to the suitable environment, the helical fibers (1D) become long and thin freely as a stable state. When reaching a certain concentration such as 1 wt% FG, gel, as a major form, displays well-ordered morphology and sensitive response in base. Through controlling the amount of base/acid, various structures (particle 0D, bamboo-like fiber 1D, flocculent membrane 2D) are generated. What's more, the intermolecular resistance and the rapid process of formation restrict the length and strength of gel at high concentration. So the fibers at 2 wt% FG look like the cluster of stumpy wire which causes the gel weak and more close to crystal.[45]

4 Conclusions:

In summary, utilizing a small bioactive molecule to construct multidimensional nanostructures and by a simple good/poor solvent procedure, we achieved the fine tuning of supramolecular structures in dimension, length, strength and shape, which may be used for bio-functional device. Nontoxic choices of assembled molecules and solvent push the study to a higher level. What's more, the mechanical properties of the gel fibers are even comparable to the covalent or polymer fibers. The results about various morphologies of self-assembly demonstrate the intermolecular interactions including hydrogen bonding, π-π stacking, hydrophile-lipophile balance and steric effects play an important role in supramolecular formation. Low-molecular-weight self-assembly with well-defined morphologies paves the way to supramolecular bioactive molecules for potential application in life area.

References:

[1] Ariga, K.; Ji, Q.; McShane, M. J.; Lvov, Y. M.; Vinu, A.; & Hill, J. P. Inorganic Nanoarchitectonics for Biological Applications. *Chem. Mater.* **2011**, *24*, 728-737.

[2] a) Yu, G.; Han, C.; Zhang, Z.; Chen, J.; Yan, X.; Zheng, B.; & Huang, F. Pillar [6] Arene-Based Photoresponsive Host–Guest Complexation. *J. Am. Chem. Soc.* **2012**, *134*, 8711-8717. b) Xu, L.; Feng, L.; Han, Y.; Jing, Y.; Xian, Z.; Liu, Z.; Yan, Y. Supramolecular Self-assembly Enhanced Europium (iii) Luminescence under Visible Light. *Soft matter* **2014**, *10*, 4686–4693.

[3] Ji, X.; Li, J.; Chen, J.; Chi, X.; Zhu, K.; Yan, X.; & Huang, F. Supramolecular Micelles Constructed by Crown Ether-Based Molecular Recognition. *Macromolecules* **2012**, *45*, 6457-6463.

[4] Guo, D. S.; Wang, K.; Wang, Y. X.; & Liu, Y.; Cholinesterase-responsive Supramolecular Vesicle. *J. Am. Chem. Soc.* **2012**, *134*, 10244-10250.

[5] a) Zhang, P.; Cheetham, A. G.; Lin, Y. A.; Cui, H. Self-assembled Tat nanofibers as effective drug carrier and transporter. *ACS nano* **2013**, *7*, 5965-5977. b) Shimizu, T.; Masuda, M.; Minamikawa, H. Supramolecular Nanotube Architectures Based on Amphiphilic Molecules. *Chem. Rev*. **2005**, *105*, 1401-1444. b) Liu, Y.; Wang, T.; Huan, Y.; et al. Self-Assembled Supramolecular Nanotube Yarn. *Adv. Mater.*, **2013**, *25*,

5875–5879.

[6] Pantoş G.; Dr. P. P.; Sanders Prof. J. Hydrogen-Bonded Helical Organic Nanotubes. *Angew. Chem*. **2006**, *119*, 198–201.

[7] Smith, A.; Williams, R.; Tang, C.; et al. Fmoc-Diphenylalanine Self Assembles to a Hydrogel via a Novel Architecture Based on π–π Interlocked β-Sheets. *Adv. Mater.* **2008**, *20*, 37–41.

[8] Cho, N. J.; Hwang, L. Y.; Solandt, J. J.; & Frank, C. W. Comparison of Extruded and Sonicated Vesicles for Planar Bilayer Self-assembly. *Materials* **2013**, *6*, 3294-3308.

[9] Estroff, L. A.; & Hamilton, A. D. Water Gelation by Small Organic Molecules. *Chem. Rev.* **2004**, *104*, 1201-1218.

[10] a) Zhao, Y. L.; & Stoddart, J. F. Noncovalent Functionalization of Single-walled Carbon Nanotubes. *Accounts. Chem. Res*. **2009**, *42*, 1161-1171. b) Ciancaleoni, G.; Di Maio, I.; Zuccaccia, D.; & Macchioni, A. Self-aggregation of Amino-acidate Half-sandwich Ruthenium (II) Complexes in Solution: From Monomers to Nanoaggregates. *Organometallics* **2007**, *26*, 489-496.

[11] Rozlosnik, N.; Gerstenberg, M. C.; & Larsen, N. B. Effect of Solvents and Concentration on the Formation of a Self-assembled Monolayer of Octadecylsiloxane on Silicon. *Langmuir* **2003**, *19*, 1182-1188.

[12] a) Caplan, M. R.; Schwartzfarb, E. M.; Zhang, S.; Kamm, R. D.; Lauffenburger, D. A. Control of Self-assembling Oligopeptide Matrix Formation Through Systematic Variation of Amino Acid Sequence. *Biomaterials* **2002**, *23*, 219-227. b) Caplan, M. R.; Schwartzfarb, E. M.; Zhang, S.; Kamm, R. D.; Lauffenburger, D. A. Effects of Systematic Variation of Amino Acid Sequence on the Mechanical Properties of a Self-assembling, Oligopeptide Biomaterial. *J. Biomat. Sci-polym. Edit.* **2002**, *13*, 225-236.

[13] Li, Z.; Zhang, H.; Zheng, W.; Wang, W.; Huang, H.; Wang, C.; & Wei, Y. Highly Sensitive and Stable Humidity Nanosensors Based on LiCl Doped TiO2 Electrospun Nanofibers. *J. Am. Chem. Soc.* **2008**, *130*, 5036-5037.

[14] a) Qiao, Y.; Lin, Y.; Yang, Z.; Chen, H.; Zhang, S.; Yan, Y.; & Huang, J. Unique

Temperature-dependent Supramolecular Self-assembly: From Hierarchical 1D Nanostructures to Super Hydrogel. *J. Phys. Chem. B* **2010**, *114*, 11725-11730. b) Bae, J.; Choi, J. H.; Yoo, Y. S.; Oh, N. K.; Kim, B. S.; & Lee, M. Helical Nanofibers from Aqueous Self-assembly of an Oligo (p-phenylene)-based Molecular Dumbbell. *J. Am. Chem. Soc.* **2005**, *127*, 9668-9669. c) Zang, L.; Che, Y.; & Moore, J. S. One-dimensional Self-assembly of Planar π-conjugated Molecules: Adaptable Building Blocks for Organic Nanodevices. *Accounts. Chem. Res.* **2008**, *41*, 1596-1608. d) Jiang, L.; Yan, Y.; & Huang, J. Versatility of Cyclodextrins in Self-assembly Systems of Amphiphiles. *Adv. Colloid. Interface.* **2011**, *169*, 13-25.

[15] a) Faul, C. F.; & Antonietti, M. Ionic Self‐assembly: Facile Synthesis of Supramolecular Materials. *Adv. Mater.* **2003**, *15*, 673-683. b) Das, D.; Dasgupta, A.; Roy, S.; Mitra, R. N.; Debnath, S.; & Das, P. K. Water Gelation of an Amino Acid‐Based Amphiphile. *Chem-Eur. J.* **2006**, *12*, 5068-5074.

[16] a) Weng, W.; Li, Z.; Jamieson, A. M.; & Rowan, S. J. Control of Gel Morphology and Properties of a Class of Metallo-supramolecular Polymers by Good/poor Solvent Environments. *Macromolecules* **2008**, *42*, 236-246. b) Lee, C. C.; Grenier, C.; Meijer, E. W.; & Schenning, A. P. Preparation and Characterization of Helical Self-assembled Nanofibers. *Chem. Soc. Rev.* **2009**, *38*, 671-683.

[17] Tian, B.; Tao, X.; Ren, T.; Weng, Y.; Lin, X.; Zhang, Y.; & Tang, X. Polypeptide-based Vesicles: Formation, Properties and Application for Drug Delivery. *J. Mater. Chem.* **2012**, *22*, 17404-17414.

[18] Yu, L.; & Ding, J. Injectable Hydrogels as Unique Biomedical Materials. *Chem. Soc. Rev.* **2008**, *37*, 1473-1481.

[19] a) Antonietti, M.; & Förster, S. Vesicles and Liposomes: a Self‐assembly Principle Beyond Lipids. *Adv. Mater.* **2003**, *15*, 1323-1333. b) Klausner, R. D.; Donaldson, J. G.; & Lippincott-Schwartz, J. Brefeldin A: Insights into the Control of Membrane Traffic and Organelle Structure. *J. Cell. Biol*. **1992**, *116*, 1071-1080. b) Liu, G., Jin, Q., Liu, X., Lv, L., Chen, C., & Ji, J. Biocompatible Vesicles based on Peo-b-pmpc/α-cyclodextrin Inclusion Complexes for Drug Delivery. *Soft Matter* **2011**, *7*, 662-669. c) Duan Q., Cao Y., Li Y., Hu X., Xiao T., Lin C., Pan Y., Wang L.

pH-Responsive Supramolecular Vesicles Based on Water-Soluble Pillar[6]arene and Ferrocene Derivative for Drug Delivery. *J. Am. Chem. Soc.* **2013**, *135*, 10542−10549. d) Wang K., Guo D., Liu Y. Temperature-Controlled Supramolecular Vesicles Modulated by p-Sulfonatocalix[5]arene with Pyrene. *Chem. Eur. J.* **2010**, *16*, 8006 - 8011.

[20] a) Qiao, Y.; Lin, Y.; Wang, Y.; Yang, Z.; Liu, J.; Zhou, J.; ... & Huang, J. Metal-driven Hierarchical Self-assembled One-dimensional Nanohelices. *Nano. Lett.* **2009**, *9*, 4500-4504. b) Lin, Y.; Qiao, Y.; Gao, C.; Tang, P.; Liu, Y.; Li, Z.; Huang, J. Tunable One-dimensional Helical Nanostructures: From Supramolecular Self-assemblies to Silica Nanomaterials. *Chem. Mater.* **2010**, *22*, 6711-6717. c) Yan, Y.; Lin, Y.; Qiao, Y.; Huang, J. Construction and Application of Tunable One-dimensional Soft Supramolecular Assemblies. *Soft. Matter*. **2011**, *7,* 6385-6398.

[21] a) Shen Z., Wang T., Liu M. Macroscopic Chirality of Supramolecular Gels Formed from Achiral Tris(ethyl cinnamate) Benzene-1,3,5-tricarboxamides. *Angew. Chem.* DOI: 10.1002/anie.201407223. b) Cao, H.; Zhu, X.; Liu, M. Self - Assembly of Racemic Alanine Derivatives: Unexpected Chiral Twist and Enhanced Capacity for the Discrimination of Chiral Species. *Angew. Chem. Int. Edit.* **2013**, *52*, 4122-4126. c) Larsen, G. K.; He, Y.; Ingram, W.; & Zhao, Y. Hidden Chirality in Superficially Racemic Patchy Silver Films. *Nano. Lett.* **2013**, *13*, 6228-6232. d) Larsen, G.; He, Y.; Ingram, W.; LaPaquette, E.; Wang, J.; Zhao, Y. P. The Fabrication of Three-dimensional Plasmonic Chiral Structures by Dynamic Shadowing Growth. *Nanoscale* **2014**, *6*, 9467-9476

[22] a) Cölfen, H.; Mann, S. Higher - order Organization by Mesoscale Self - assembly and Transformation of Hybrid Nanostructures. *Angew. Chem. Int. Edit.* **2003**, *42*, 2350-2365. b) Miguel C., Antoni S., José L., et al. Supramolecular Architectures from Bent-Core Dendritic Molecules. *Angew. Chem.* DOI: 10.1002/anie.201407705. c) Xing, P., Chu, X., Ma, M., Li, S., & Hao, A. Melamine as an effective supramolecular modifier and stabilizer in a nanotube-constituted supergel. *Chem – Asian. J.* DOI: 10.1002/asia.201402645.

[23] Liu, J.; Huang, X.; Li, Y.; Sulieman, K. M.; He, X.; & Sun, F. Hierarchical

Nanostructures of Cupric Oxide on a Copper Substrate: Controllable Morphology and Wettability. *J. Mater. Chem.* **2006**, *16*, 4427-4434.

[24] a) Zhao, Y.; Beck, J. B.; Rowan, S. J.; Jamieson, A. M. Rheological Behavior of Shear-responsive Metallo-supramolecular Gels. *Macromolecule* **2004**, *37*, 3529-3531. b) Yang, Z.; Liang, G.; Wang, L.; Xu, B. Using a Kinase/phosphatase Switch to Regulate a Supramolecular Hydrogel and Forming the Supramolecular Hydrogel in Vivo. *J. Am. Chem. Soc.* **2006,** *128*, 3038-3043.

[25] Eyrich, D.; Brandl, F.; Appel, B.; Wiese, H., Maier, G.; Wenzel, M.; Blunk, T. Long-term Stable Fibrin Gels for Cartilage Engineering. *Biomaterial* **2007**, *28*, 55-65.

[26] Thim, L.; Madsen, F.; Poulsen, S. S. Effect of Trefoil Factors on the Viscoelastic Properties of Mucus Gels. *Eur. J. Clin. Invest.* **2002**, *32*, 519-527.

[27] Semerdzhiev, S. A.; Dekker, D. R.; Subramaniam, V.; Claessens, M. M. Self-Assembly of Protein Fibrils into Supra-Fibrillar Aggregates: Bridging the Nano-and Mesoscale. *ACS nano*. **2014**, *8*, 5543–5551.

[28] Bobrovsky, A.; Shibaev, V.; Bubnov, A.; Hamplová, V.; Kašpar, M.; Glogarová, M. Effect of Molecular Structure on Chiro-Optical and Photo-Optical Properties of Smart Liquid Crystalline Polyacrylates. *Macromolecules* **2013,** *46*, 4276-4284.

[29] Liu, H.; Yang, Z.; Meng, L.; Sun, Y.; Wang, J.; Yang, L.; Tian, Z. Three-Dimensional and Time-Ordered Surface-Enhanced Raman Scattering Hotspot Matrix. *J. Am. Chem. Soc.* **2014**, *136*, 5332-5341.

[30] Xu, S.; Lin, Y.; Huang, J.; Li, Z.; Xu, X.; Zhang, L. Construction of High Strength Hollow Fibers by Self-assembly of a Stiff Polysaccharide with Short Branches in Water. *J. Mater. Chem. A* **2013**, *1*, 4198-4206.

[31] a) Yu, G.; Yan, X.; Han, C.; Huang, F. Characterization of Supramolecular Gels. *Chem. Soc. Rev.* **2013,** *42*, 6697-6722. b) Yu, X.; Chen, L.; Zhang, M.; Yi, T. Low-molecular-mass Gels Responding to Ultrasound and Mechanical Stress: Towards Self-healing Materials. *Chem. Soc. Rev.* **2014**, *43*, 5346-5371

[32] Xing, P.; Chu, X.; Ma, M.; Li, S.; Hao, A. Supramolecular Gel from Folic Acid with Multiple Responsiveness, Rapid Self-recovery and Orthogonal Self-assemblies. *Phys. Chem. Chem. Phys.* **2014**, *16*, 8346-8359.

[33] Wang, L.; Yang, X.; Chen, H.; Gong, T.; Li, W.; Yang, G.; Zhou, S. Design of Triple-Shape Memory Polyurethane with Photo-cross-linking of Cinnamon Groups. *ACS Appl. Mater. Inter.* **2013**, *5*, 10520-10528.

[34] Xing P.; Chu X.; Li S. Hybrid Gels Assembled from Fmoc–Amino Acid and Graphene Oxide with Controllable Properties. ChemPhysChem **2014**, *15*, 2377-2385.

[35] Gupta, G.; Iyer, S.; Leasure, K.; Virdone, N.; Dattelbaum, A. M.; Atanassov, P. B.; López, G. P. Stable and Fluid Multilayer Phospholipid–silica Thin Films: Mimicking Active Multi-lamellar Biological Assemblies. *ACS nano*. **2013**, *7*, 5300-5307.

[36] Datar, A.; Balakrishnan, K.; Zang, L. One-dimensional Self-assembly of a Water Soluble Perylene Diimide Molecule by pH Triggered Hydrogelation. *Chem. Commun.* **2013**, *49*, 6894-6896.

[37] Sivadas, A. P.; Kumar, N. S.; Prabhu, D. D.; Varghese, S.; Prasad, S. K.; Rao, D. S.; Das, S. Supergelation via Purely Aromatic π–π Driven Self-Assembly of Pseudodiscotic Oxadiazole Mesogens. *J. Am. Chem. Soc.* **2014**, *136*, 5416-5423.

[38] Mai, Y.; Xiao, L.; Eisenberg, A. Morphological Control in Aggregates of Amphiphilic Cylindrical Metal–Polymer "Brushes". *Macromolecules* **2013**, *46*, 3183-3189.

[39] Hou, Y.; Gao, L.; Feng, S.; Chen, Y.; Xue, Y.; Jiang, L.; Zheng, Y. Temperature-triggered Directional Motion of Tiny Water Droplets on Bioinspired Fibers in Humidity. *Chem. Commun.* **2013**, *49*, 5253-5255.

[40] a) He, X.; Lin, J. B.; Kan, W. H.; Dong, P.; Trudel, S.; Baumgartner, T. Molecular Engineering of "Click" ‐ Phospholes Towards Self ‐ Assembled Luminescent Soft Materials. *Adv. Funct. Mater.* **2014**, *24*, 897-906. b) Fei, J.; Gao, L.; Zhao, J.; Du, C.; Li, J. Responsive Helical Self ‐ Assembly of AgNO3 and Melamine Through Asymmetric Coordination for Ag Nanochain Synthesis. *Small* **2013**, *9*, 1021-1024.

[41] a) Chen, L.; Mali, K. S.; Puniredd, S. R.; Baumgarten, M.; Parvez, K.; Pisula, W.; Müllen, K. Assembly and Fiber Formation of a Gemini-type Hexathienocoronene Amphiphile for Electrical Conduction. *J. Am. Chem. Soc.* **2013**, *135*, 13531-13537. b) Laird, E. D.; Li, C. Y. Structure and Morphology Control in Crystalline Polymer–carbon Nanotube Nanocomposites. *Macromolecules* **2013**, *46*, 2877-2891.

[42] Westerlund, F.; Lemke, H. T.; Hassenkam, T.; Simonsen, J. B.; Laursen, B. W. Self-Assembly and Near Perfect Macroscopic Alignment of Fluorescent Triangulenium Salt in Spin-Cast Thin Films on PTFE. *Langmuir* **2013**, *29*, 6728-6736.

[43] Wang, K.; Guo, D. S.; Wang, X.; Liu, Y. Multistimuli Responsive Supramolecular Vesicles Based on the Recognition of p-sulfonatocalixarene and its Controllable Release of Doxorubicin. *ACS nano* **2011**, *5*, 2880-2894.

[44] Mignon, P.; Loverix, S.; Steyaert, J.; Geerlings, P. Influence of the π–π interaction on the Tydrogen Bonding Capacity of Stacked DNA/RNA Bases. *Nucleic. Acids. Res.* **2005**, *33*, 1779-1789.

[45] a) Shalkevich, A.; Stradner, A.; Bhat, S. K.; Muller, F.; Schurtenberger, P. Cluster, Glass, and Gel Formation and Viscoelastic Phase Separation in Aqueous Clay Suspensions. *Langmuir* **2007**, *23*, 3570-3580. b) Chou, C. M.; Hong, P. D. Nucleation, Growth, Fractal Aggregation, and Late-stage Coarsening on Structural Development of Polymer Physical Gels. *Macromolecules* **2004**, *37*, 5596-5606.